Finding Exoplanets from Your Driveway

A friend and fellow Halifax RASC Centre member joined me on December 9, 2025 to see if we could observe a transit of HD189733b in front of its parent star. As this was the first attempt to observe the exoplanet transit, it was treated as a bit of an experiment. The first lesson, everything takes longer than expected so start early. Due to an alignment star being in the trees, it took longer to get the system aligned and the start of the transit was missed by several minutes!

Despite observing from a less than ideal urban location, the exoplanet transit was clearly detected meeting the experiment's primary goal. In addition, using the data collected, other aspects of HD 189733b were explored such as the existence of an atmosphere.

The Star System

HD189733 is a 7.8 magnitude yellow-orange star in Vulpecula with a transiting exoplanet known as HD189733b, approximately 63 light years from Earth.

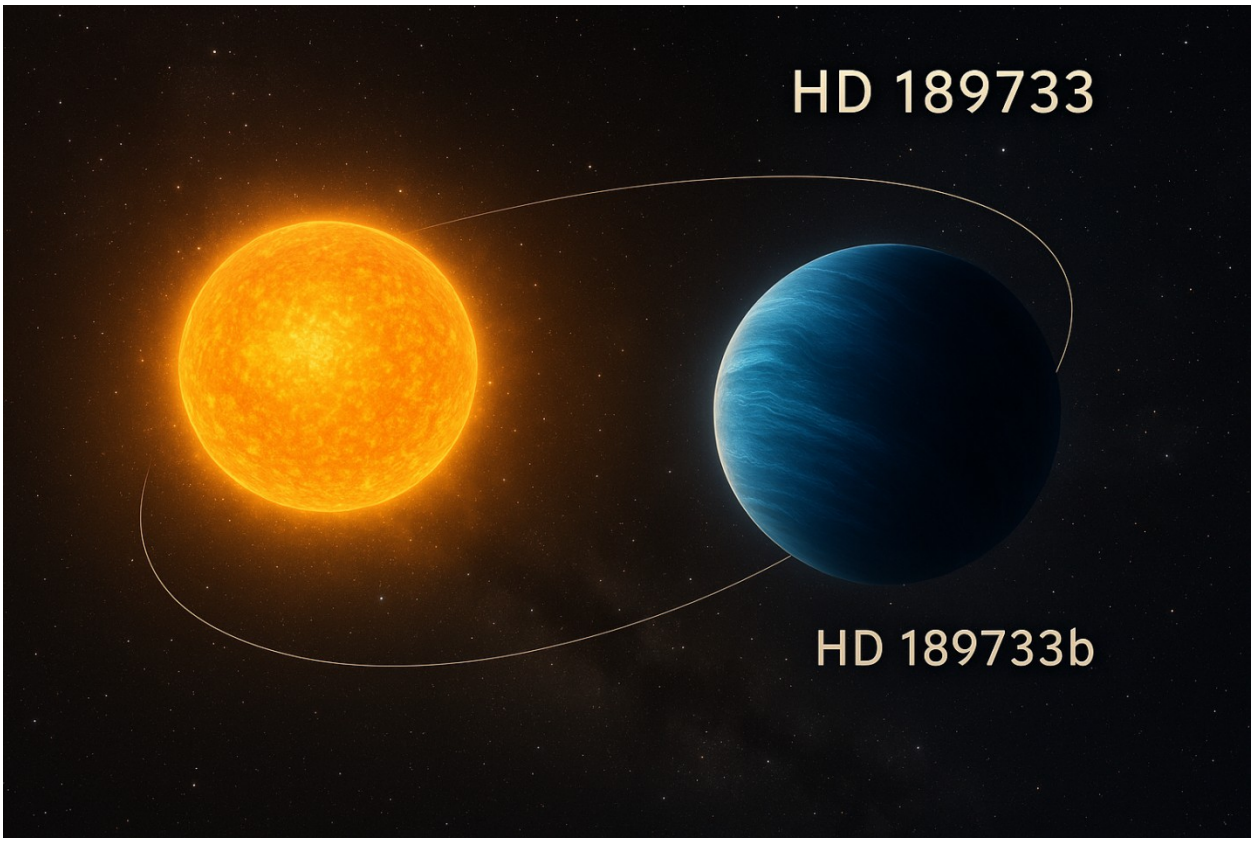

Figure 1 - Graphical representation of the HD189733 system.

HD189733b is a hot Jupiter type gas giant and orbits approximately 4.6 million km from its star. It completes one orbit every 2.2 days and the light curve dips about 2% at mid transit. The star is in the center of the image below, with M27 to the right. The field is 1.5 degrees by 1 degree.

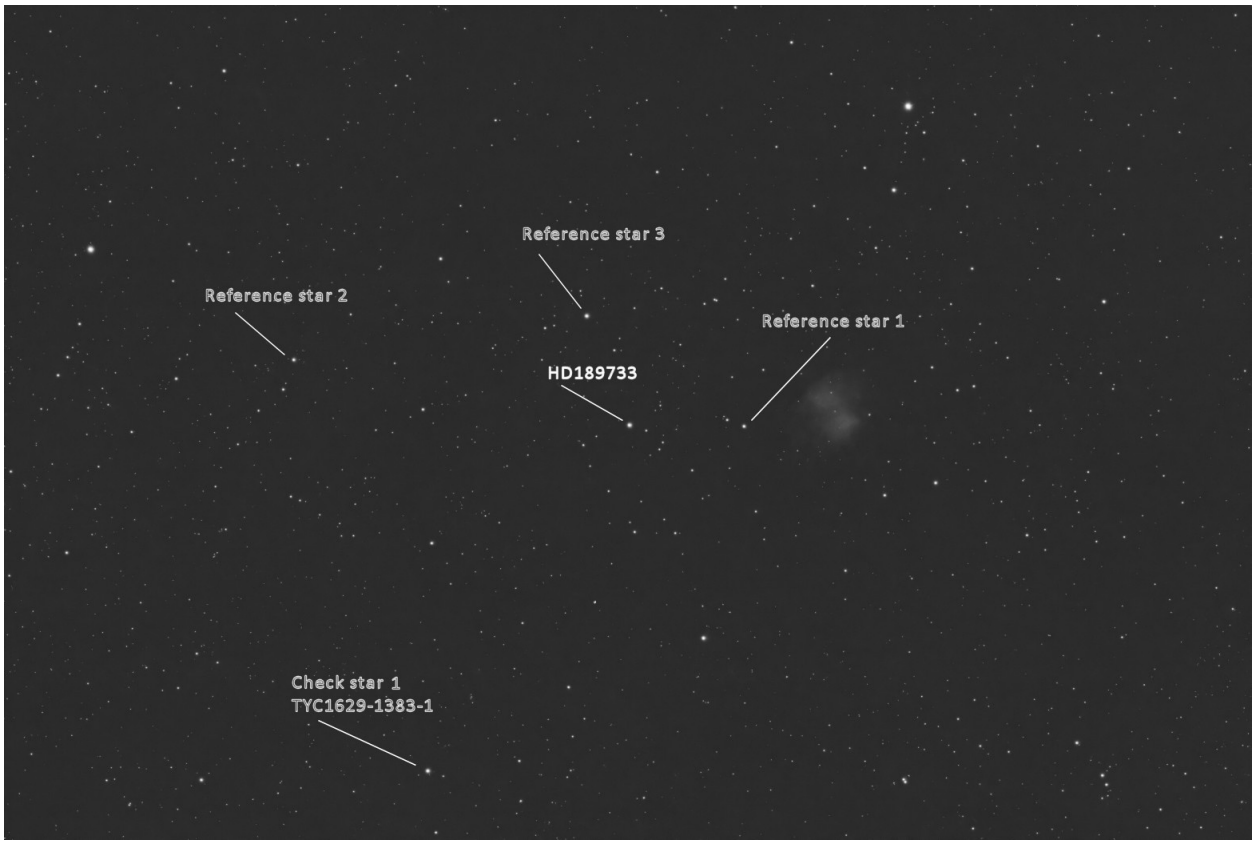

Figure 2 - The field surrounding HD189733 showing the location of the star relative to M27 as well as the locations of the reference stars and a star used to check for systematic errors.

The brightness of the star, and the relatively large mid-transit dip, puts it within the range of the equipment used.

Equipment

The equipment used for the observation consisted of a Zwo ASI2600MC Pro colour camera coupled to a SkyWatcher Esprit 120 telescope riding on a Celestron CGX-L mount. During the data acquisition, the system was guided by an Orion Star Shoot Autoguider (SSAG) coupled to a 400 mm refractor. Since the equipment usually operates at the end of a driveway, either at home or the cottage, it has been named the Driveway's End Observatory (DEO).

The Zwo camera is a modern CMOS one shot colour (OSC) camera based on the Sony IMX-571 colour sensor and was cooled to -10^0 C during data acquisition. It has very low dark current and uses a 16 bit analog to digital converter (ADC).



Figure 3 - DEO set up at a dark sky site.

Observing Site

All data was gathered under less than ideal conditions from an urban driveway in Bedford Nova Scotia. Light pollution from street lights and bright urban Bortle 6 to 7 skies limit the photographic stellar brightness to about magnitude 17.



Figure 4 - Urban observing site where the data was captured. In addition to the lights shown in this picture there were Christmas lights as well. By the end of the observing session the target was setting between the two houses almost at the tree line.

The bright sky causes a lot of photon noise and an experiment was carried out about four weeks earlier to determine the longest exposure that could be used without saturating any stars in the frame. It was found that a 1.5 second exposure produced an output of about 28000 out of a maximum of 65535 for the target star. Care was taken in selecting the reference stars to avoid any saturation while keeping the signal to noise ratio as high as possible.

Data Collection

Using the *Swarthmore College exoplanet transit calculator*, (*Jensen E. L. N. 2013. Tapir: A Web Interface for Transit/Eclipse Observability, Astrophysics Source Code Library ascl:1306.007*) transit times for December 9, 2025 were found with a favourable transit starting just before 6:30 PM AST.

Only 1 target matches your constraints (on name, V mag, depth, etc.). Searching for observable transits over 7.0 days...

Upcoming events for the next 5 days and the past 2 days from 12-09-2025; start/end given in timezone UTC.

Night starts/ends at nautical twilight.

Results shown for Other Site latitude = 44.71006, longitude = -63.68678930378416.

Colored text indicates a part of the transit that is during daylight, or a transit at elevation less than the user-specified limits, or that the Moon is relatively full and close to the target.

Click on column headers to sort the table by that column. Click again to reverse the sorting order. To sub-sort, first click one column (e.g. the left-hand one to sort by night), then *shift-click* another column to sort further within the first category. For example, to sort by priority within a given night (when multiple nights are displayed), first click the "Local evening date" header, then shift-click the "Priority" header. The highlighted column shows the current sorting.

The buttons can be used to toggle the visibility of columns, and the column order can be rearranged by clicking and dragging the column header.

Column visibility | Reset column order | Show all columns | Disable tooltips

Search: | Show if visible transit % + baseline % > 0 | V_{max}: | $Depth_{min}$: 0 ppt | Overlap: 0 m. | Other Site

Local evening date	Name	V or Gaia mag	Start—Mid—End	Duration	BJD_{TDB} start-mid-end	Elev. at start, mid, end ±1 hrs	% of transit (baseline) observable, Suggested obs. start, end	Az. at start, mid, end ±1 hrs	HA at start, mid, end ±1 hrs	RA & Dec (J2000)	Period (days)	Depth (ppt)	Comments
Tue. 2025-12-09: Nautical twilight 2025-12-09 21:44 — 2025-12-10 10:30 local time / 2025-12-09 21:44 — 2025-12-10 10:30 UTC													
Tue. 2025-12-09 Nautical twilight 21:44 – 10:30 (UTC)	☐ HD 189733 b Finding charts: Annotated, Aladin, SkyMap; Airmass plot, ACP plan Info: Exoplanet Archive, Simbad, Gaia, TIC	7.7 Moon 69% @134°	21:22 22:22—23:17—00:11 01:11 ±0:00	1:49	11019.4302 11019.4681 11019.5060	54° 44°, 34°, 24° 14°	100% (82%) 21:44—01:11	244° 259°, 269°, 279° 288°	+2.3 +3.4, +4.3, +5.2 +6.2	20:00:43.71 +22:42:35.19	2.22	24.0	Ephemeris from Kokori et al. 2023.

Showing 1 to 1 of 1 entries

Script took 1 second for 1 events.

Figure 5 - Output of the exoplanet transit calculator at https://astro.swarthmore.edu/transits/.

The data was collected then flats, darks, and flat darks were obtained after the transit was complete. During the transit, HD189733 descended between the two houses visible in Figure 4 ending up at the tree line by the end of the transit. This increasing air mass, the amount of Earth's atmosphere through which the starlight must pass, had an impact on the data quality, reducing the signal to noise (SNR) during observing run as shown below.

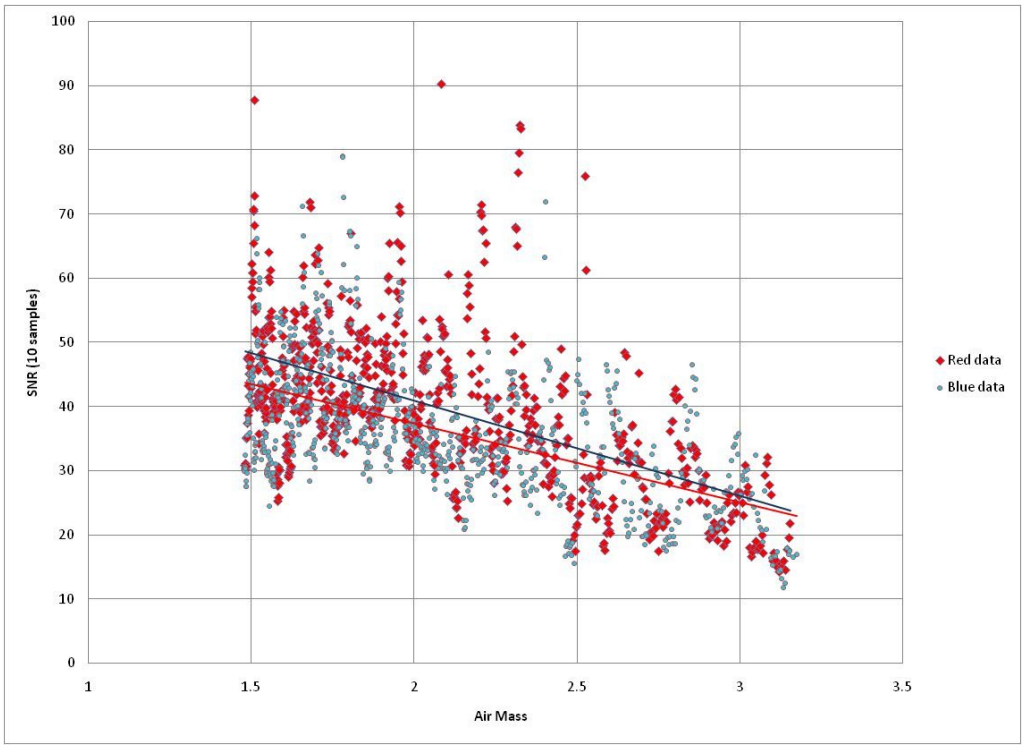

Figure 6 – HD189733 SNR versus air mass during the observation. The lowering SNR impacted the data during the later stages of the transit. The red data is simply the red channel of the OSC camera while the blue data is the blue channel.

Data Reduction & Results

In all, 783 images were obtained and each image calibrated with darks, flats, and flat darks. Following de-Bayering, the colour images were split into red green and blue monochrome images. The photometry script in *PixInsight* was used to conduct aperture photometry on each image producing red and blue flux tables in comma separated variables (CSV) format. The table contains the timestamp of the image, the V and B magnitudes, as read from the Tycho2 catalog, the position, catalog number, and the measured ADC output for each star found in the image.

As there was very little information on the red magnitude of the stars used in the data reduction, the R magnitude was estimated from the V and B values using $R = V - 0.587 \cdot (B - V) - 0.011$. This comes from estimating the star colour, and thus temperature, from the B-V colour index. A simple web search will turn up a host of mathematical formulae, all in the same form with different constants, and the formula used was chosen as it best fit the limited red data available on several stars in the image field. It should be noted that the accuracy of this empirical formula drops off as B-V becomes greater than 1.2.

Initial checks were carried out to validate the data and to look for any indication of the transit. The raw data, measured in ADC counts (simply the value of the ADC from 0 to 65535) from the camera, represent the values captured directly by the camera and extracted using the PixInsight photometry script. For those interested in more correct units, the camera gain was 0.25 e/ADU, its quantum efficiency is about 0.8 and each exposure was 1.5 seconds. The collected data clearly shows the effects of atmospheric extinction as the air mass was steadily climbing throughout observation causing the collected starlight to decrease in intensity during the data collection as shown below in Figure 7.

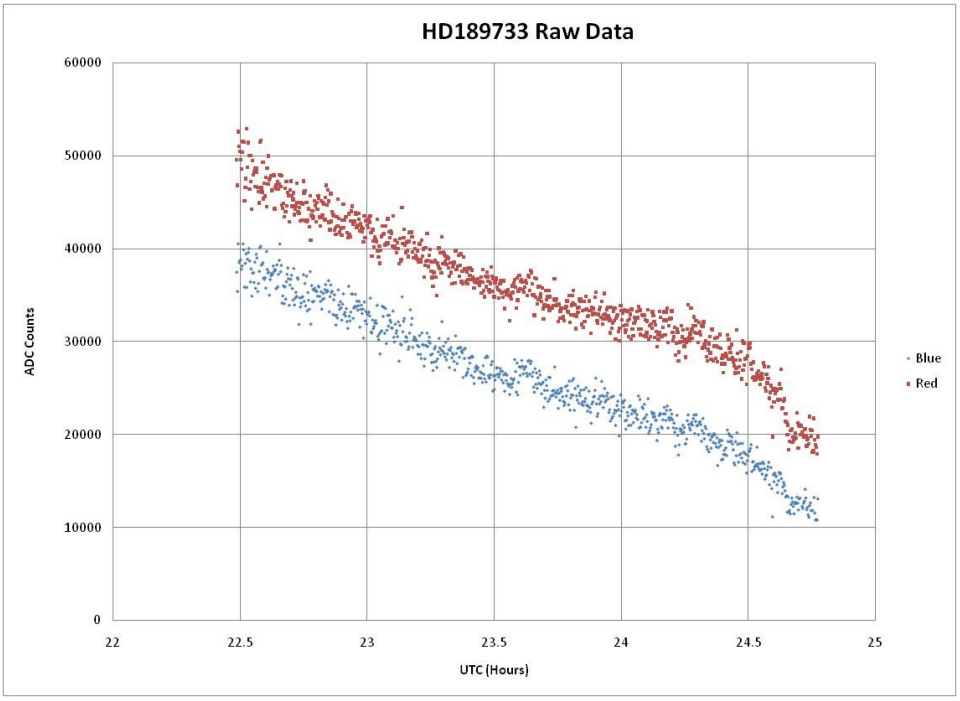

Figure 7 - Raw data from the target star collected during the observation. The downward slope is caused by atmospheric extinction.

These effects of atmospheric extinction could be corrected by applying the appropriate first order extinction corrections to the data; however, as differential photometry was used, the first order effects of loss due to extinction are cancelled out when the ADC value of the target star is divided by the ADC value of the reference star. The plot shown in Figure 8 shows the ADC counts received from the first reference star, note that it also shows a slope due to extinction effects.

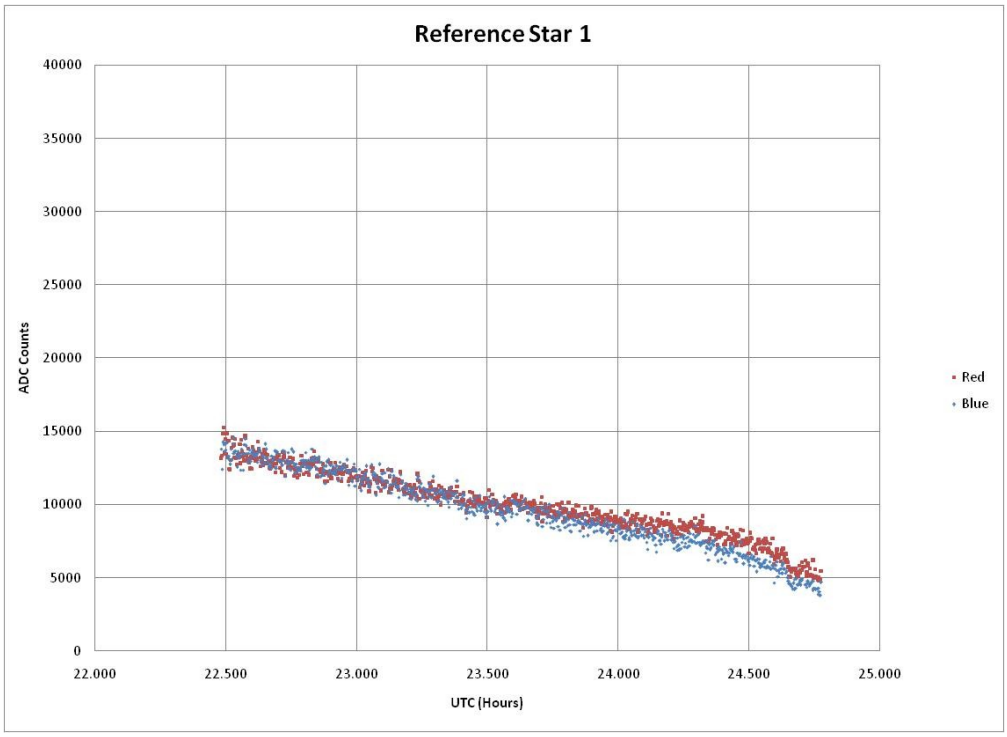

Figure 8 - Raw data from the first reference star collected during the observation. The downward slope is similar to that seen in Figure 7.

The target star (S_t) differential ADC values are calculated from $\Delta S_t = \frac{S_t}{S_{ref}}$ (Eq1).

Where: S_t is the measured brightness (ADC value) of the target star
S_{ref} is the measured brightness (ADC value) of the reference star

Plotting ΔS_t against time shows that using the differential ADC value, most of the atmospheric extinction effects are removed as they cancel in the division.

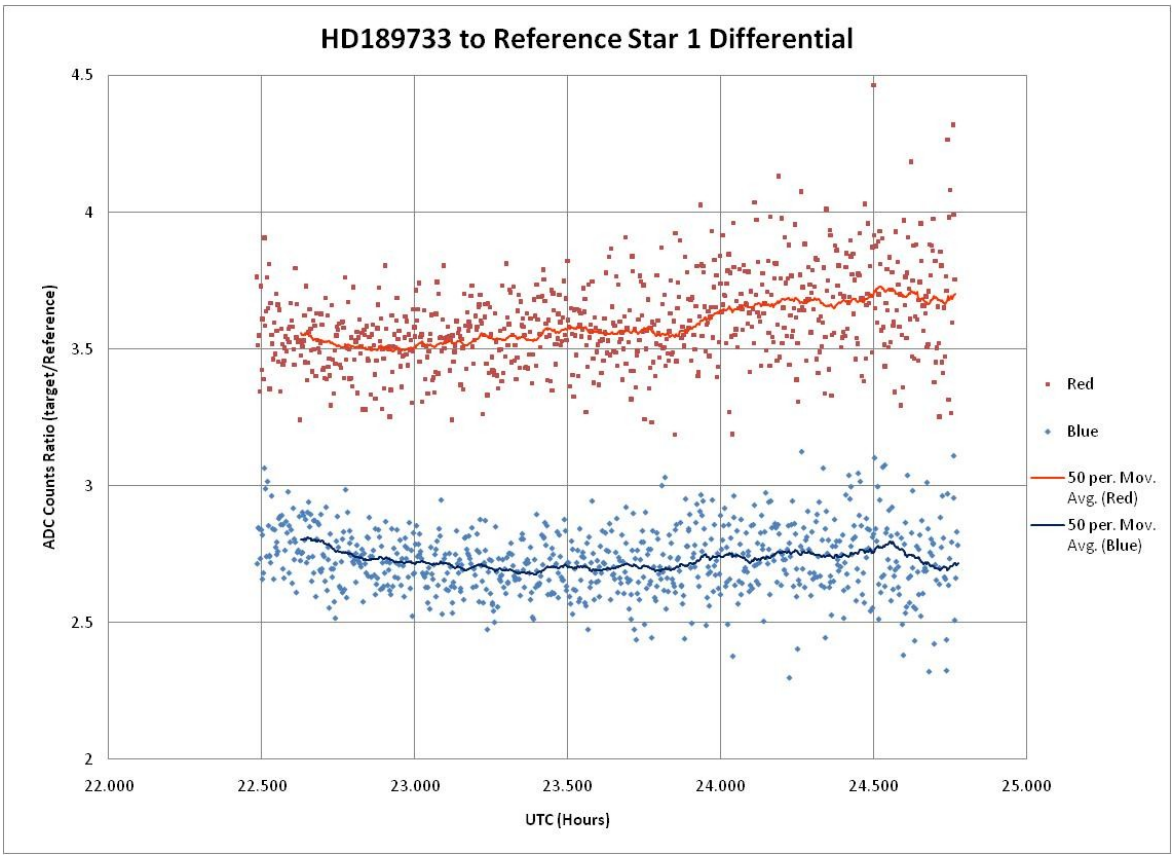

Figure 9 - Differential data easily showing the transit in the red channel.

The moving average of the red channel differential data shows the transit ending around 00:20 UTC (the hour count was allowed to exceed 24 for purposes of the plotting program). The data also shows that the start of the transit was missed by a few minutes. The moving average filter, used to smooth the data in Figure 9, is less than optimal as it puts an *n* sample delay in the output, where *n* is the number of samples used in the moving average. The data was re-smoothed using an adaptive symmetric nearest neighbour linear least-squares fit algorithm that gives better smoothing with minimal delay. In addition, three estimates of the brightness, each using different reference stars were averaged to reduce the noise in the data resulting in the plot shown in Figure 10.

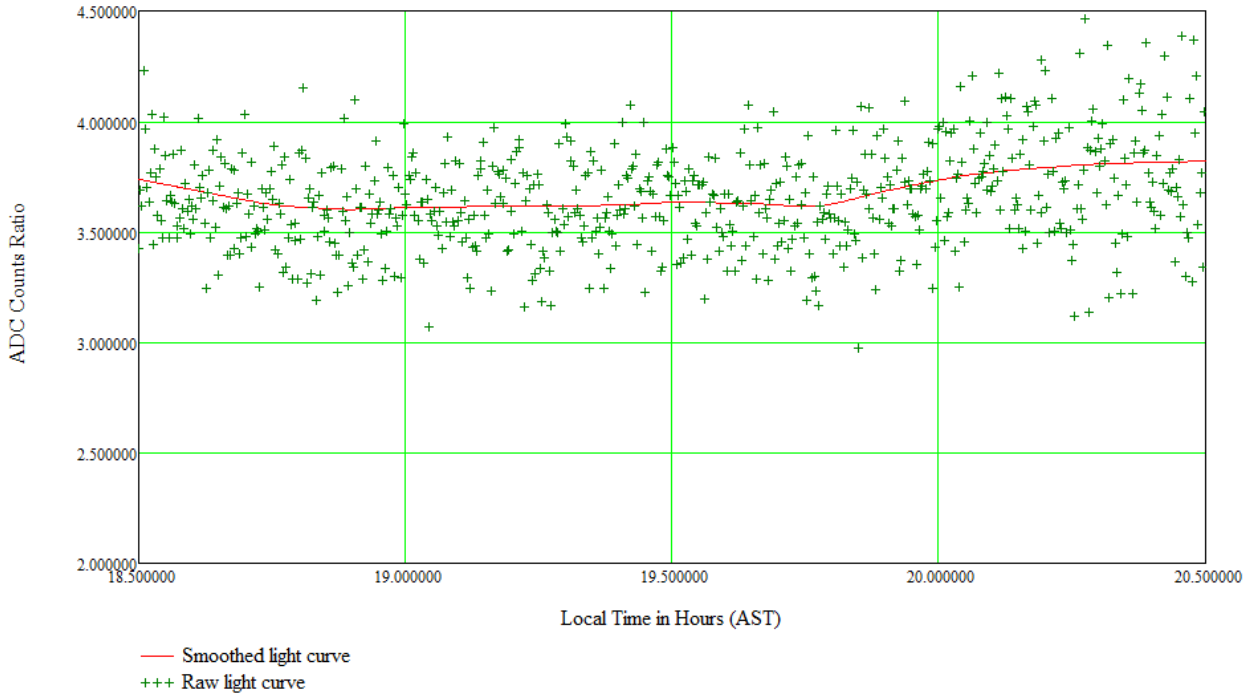

Figure 10 - Averaged data with an adaptive smoothing filter makes the transit clearly visible.

This approach is clearly superior to the simple moving average and is used for all smoothed data plots unless otherwise noted. With the data verified, and knowing that it contains the transit, the rest of the data reduction was carried out.

Atmospheric extinction affects blue stars more than red stars as noted in *The Cepheid impostor HD 18391 and its anonymous parent cluster* by *D.G. Turner, V.V. Kovtyukh, D.J. Majaess, D.J. Lane, and K.E. Moncrieff* published in Astronomical Notes in 2009. There are also differences caused by where the starlight falls within the bandpass of the colour filter. These effects are not corrected using differential techniques and need to be removed from the data. The second order extinction coefficients ks_b and ks_{br}, were measured using the technique outlined in the *Workbook for Astronomical Photoelectric Photometry (ISBN 0-9628592-1-4)* and used to complete the correction for atmospheric extinction. Tracking a red and a blue star throughout the observing session and plotting the observed colour index against the colour index times the air mass allowed the calculation of the required coefficients to remove extinction effects. Note that the colour index coefficient is ks_{br}, not k_{bv}, as the colour filters were not standard UBV filters. The filters were, in fact, the Bayer RGB filters of the Zwo OSC camera. Because of this, and because it was not necessary for the purpose of obtaining evidence of the transit, no effort was put toward transforming the data to a standard system, short of removing the extinction effects. The approximate combined QE and filter response of the Zwo camera is shown in Figure 11. Although not an exact match for proper photometric filters, it is not too far off.

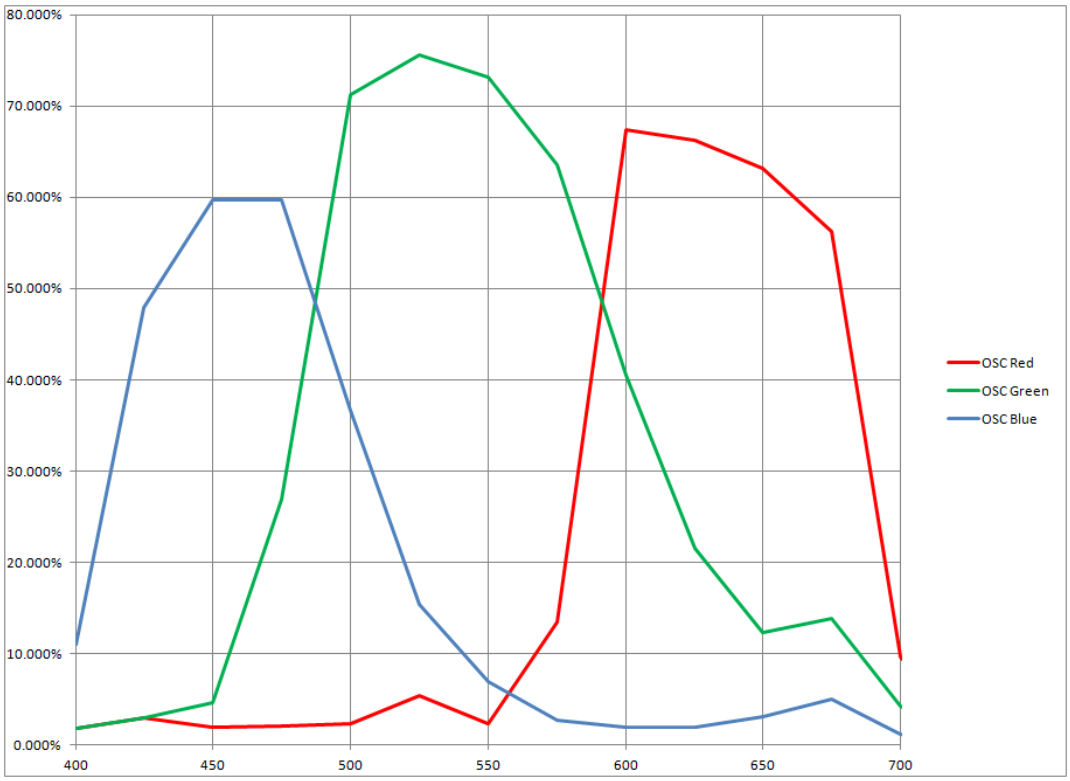

Figure 11 - Zwo camera colour filter response. This plot takes the quantum efficiency and the optical window of the camera into account.

After the coefficients were determined, the magnitude of the target star was calculated using

$$S_{tmag} = S_{ref_mag} - 2.5 \cdot \log\left(\frac{S_t}{S_{ref}}\right) - ks \cdot \Delta(b - r) \cdot X \quad \text{(Eq2)}.$$

Where: S_t is the measured brightness of the target star

S_{ref} is the measured brightness of the reference star

S_{ref_mag} is the magnitude of the reference star from the Tycho2 catalog

ks is the second order extinction coefficient for the colour channel

Δ(b-r) is the difference in colour index of the target and reference stars

X is the air mass

Three separate magnitudes were calculated using three different reference stars (Figure 2).

Next, the three target magnitudes were averaged to reduce the noise in the data using

$$S_{tavg} = -2.5 \log\left(\frac{\frac{S_{t1}}{10^{-2.5}} + \frac{S_{t2}}{10^{-2.5}} + \frac{S_{t3}}{10^{-2.5}}}{3}\right) \quad \text{Eq3}.$$

Where: S_{t1}, S_{t2}, and S_{t3} are the target magnitude estimates made using each reference star and Eq2.

The above calculations were done for the red and blue colour channels and represent the corrected instrumental magnitude as measured above the Earth's atmosphere. Finally the data was converted back to a linear brightness and both the red and blue channels normalized to their respective maximums, then the plot of the transit was produced.

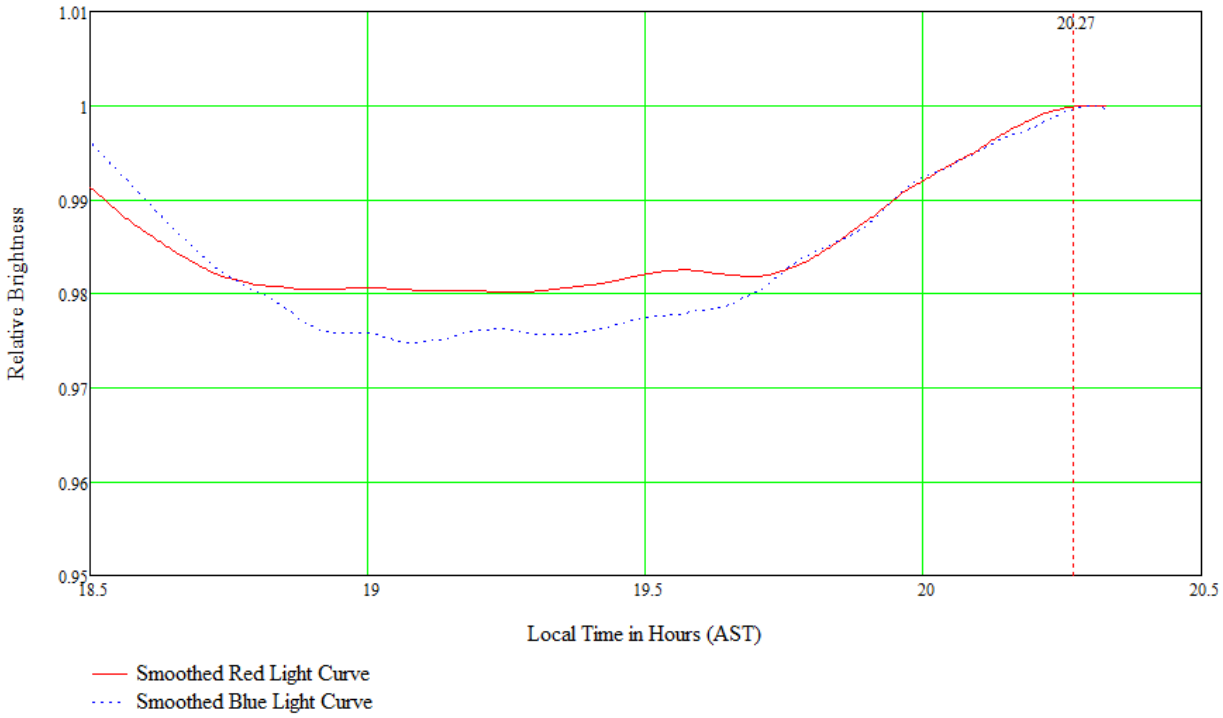

Figure 12 - Red and blue normalized light curves for HD189733 after correction for atmospheric extinction. The end of the transit is marked by the dashed red vertical line.

The data plotted in Figure 12 agrees well with measurements published by Gardner-Watkins et al. - *A Six Year, Low-resolution, Multibroadband Transit Photometry Study of HD 189733b* published in The Astronomical Journal, 165:5 (18pp), 2023 January

Table 1 - DEO data compared to Gardner-Watkins Study

Colour	Gardner-Watkins	DEO Data
Red depth	0.025	0.020
Blue depth	0.028	0.024
Δ(Blue- Red)	0.003	0.004

The authors would like to thank Dr. David Turner (RASC Halifax) for suggesting that corrections for atmospheric extinction be applied to the data. This substantially improved the agreement with the Gardner-Watkins results.

If a planet has an atmosphere Rayleigh scattering due to particulates in the clear upper layers attenuate blue light more than red. This is one of the key detectable indicators that an exoplanet has an

atmosphere. Since the camera used is a one shot colour unit, red and blue light are captured simultaneously. This opens up an interesting possibility of using very broad band spectroscopy for planetary atmosphere detection. Examining the plots of Figure 12 shows this technique can be useful as there is clear evidence that blue light has been attenuated more than red, indicating that HD189733b does indeed have an atmosphere.

As a final check on the data, the same exercise was carried out on the check star shown in Figure 2 to see if it also showed any sign of the transit. If it did then there may have been a problem with the reference stars chosen, calling the transit detection into question. Figure 13 shows the check star light curve has a residual variation that does not match that of HD189733.

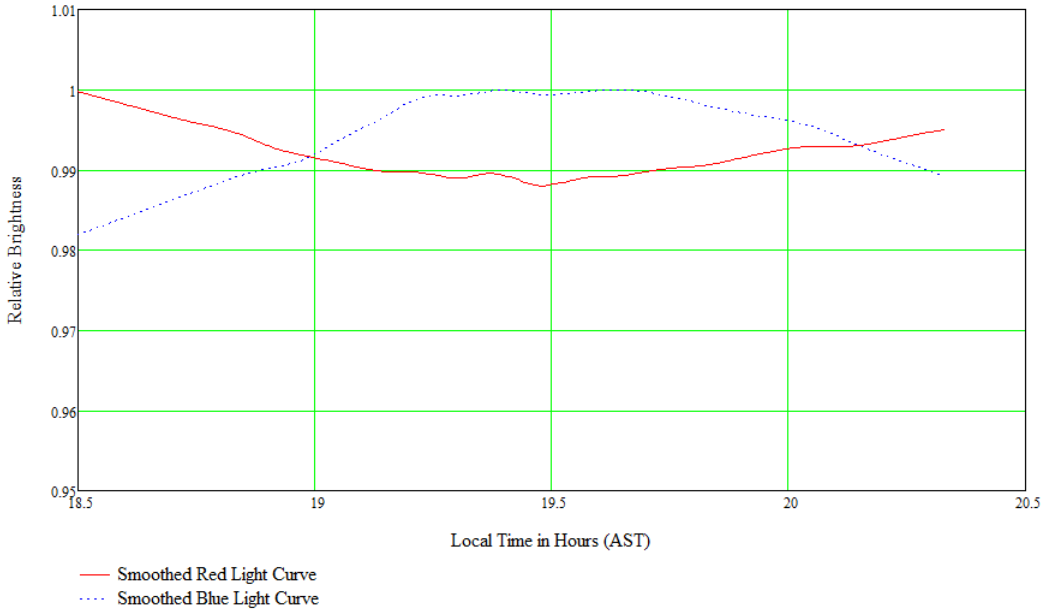

Figure 13 - Normalized light curves for the check star.

Using the end of transit (EOT) time, shown in Figure 12 and the barycentric Julian EOT time from Figure 5 it is possible to estimate the distance from Earth to the Sun on the date of the observation.

Figure 14 shows how the problem is set up.

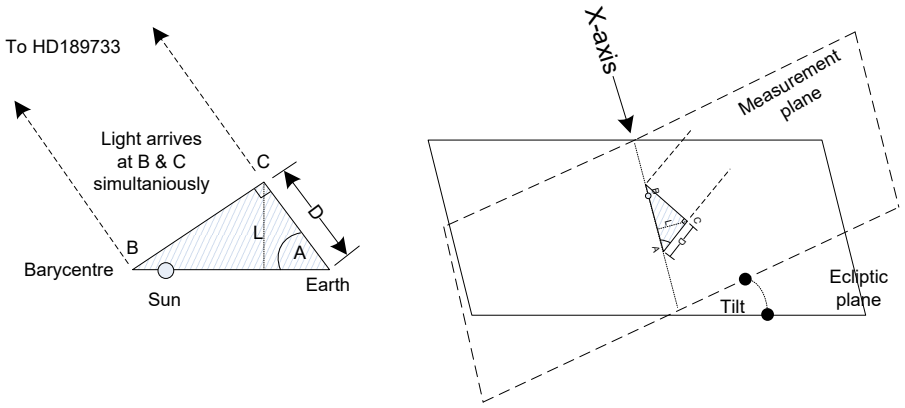

Figure 14 - Calculating the Earth-Sun distance.

The general idea is that the angle A and distance D can be used with some simple trig to calculate the Earth to barycentre distance $D_{Earth\text{-}barycentre}$=D/cos(A) Eq4. Since the barycentre lay beyond the Sun, as seen from Earth during December, the Sun to barycentre distance can be subtracted to give the Earth Sun distance. A'', the angle between the Sun and HD189733 as seen from the Earth, is measured along the equatorial plane, not the plane in which the distance D is measured. This angle is 43.42 degrees (*courtesy of the ECU planetarium program by the late Dr. David J. Lane*) and must first be projected on the ecliptic plane using $A_{TiltedPlane} = \operatorname{atan}\left(\frac{\tan(\theta_{ReferencePlane})}{\cos(tilt)}\right)$ Eq 5, where theta is the angle measured on the reference plane and tilt is the angle between the tilted and reference planes. The tilt of the ecliptic relative to the equatorial plane is 23.4393 degrees yielding an angle A'=45.886 degrees. Next, the plane of the distance measurement is defined with its X-axis being the Earth-Sun line on the ecliptic and tilted around the Earth-Sun line by the ecliptic latitude of HD189733 which is 42.175 degrees. This plane contains the Sun, the Earth, the barycentre and HD189733 and is the plane along which the transit timing is measured as it contains the direct light path from the star to the Earth. Figure 14 shows this arrangement, but the angle A' now needs to be projected from the ecliptic to this tilted measurement plane, again using equation 5, yielding a final angle A of 54.302 degrees. The distance, D, is calculated from the EOT time predicted at the barycentre, from Figure 5, and the measured EOT time as read from Figure 12. Taking the difference of these two times and multiplying by the speed of light in a vacuum yields the distance D = 89,637,944.94 km. Applying equation 4 to this using the projected angle gives the Earth to barycentre distance of 153,618,081 km. Finally the barycentre to Sun distance of 820,000 km is subtracted, as the barycentre was behind the Sun from the Earth's perspective, giving an Earth-Sun distance of 152,798,081 km. The actual Earth-Sun distance was found using the solar distance calculator (https://dqydj.com/solar-distance-calculator/) to be 147,338,091 km, an error of just 3.7%.

Conclusions

An experiment was conducted to determine if it was possible to detect the transit of an exoplanet with a small telescope and a commercially available amateur CMOS camera from a very light polluted urban environment. Not only is it possible, but the data is of high enough quality to gain insight into the exoplanetary system. The transit timing measurement allows the estimation of the Earth Sun distance to a surprising accuracy of better than four percent. The measurement seems to be resistant to noise in the data even though the EOT time happens when the measurement SNR is at its lowest. Indeed the biggest source of error is likely the reading of the EOT time from Figure 12.

The detection of an exoplanet, the detection of an exoplanet atmosphere and a measurement of the Earth Sun separation, not bad for a five inch telescope under urban skies!